A multi-proxy record of abrupt cooling events during the Windermere Interstadial at Crudale Meadow, Orkney, UK

Christopher Francis, Stefan Engels, Ian Matthews, Adrian Palmer, Rhys Timms, Anne-lise Jourdan, Ian Candy

JOURNAL OF QUATERNARY SCIENCE (2021) **36**(3) 325–338 ISSN 0267-8179. DOI: 10.1002/jqs.3289

JQS Journal of Quaternary Science QRA Quaternary Research Association

A multi-proxy record of abrupt cooling events during the Windermere Interstadial at Crudale Meadow, Orkney, UK

CHRISTOPHER P. FRANCIS,[1]* STEFAN ENGELS,[2] IAN P. MATTHEWS,[1] ADRIAN P. PALMER,[1] RHYS G. O. TIMMS,[1] ANNE-LISE JOURDAN[3] and IAN CANDY[1]

[1]Department of Geography, Royal Holloway University of London, Egham, Surrey, UK
[2]Department of Geography, Birkbeck University of London, London, UK
[3]Department of Earth Sciences, University College London, London, UK

Received 15 October 2020; Revised 8 February 2021; Accepted 9 February 2021

ABSTRACT: Three clearly defined abrupt cooling events (ACEs) can be observed within Greenland Interstadial (GI)-1 in the Greenland ice-core records. However, the spatial variation in amplitude and timing of these ACEs is poorly understood due to the paucity of well-dated records with quantified temperature reconstructions. This study presents high-resolution chironomid-inferred July air temperature (T_{Jul}) and oxygen isotope ($\delta^{18}O$) records from Crudale Meadow (Orkney Isles, UK). Three centennial-scale ACEs punctuate the Windermere Interstadial at Crudale Meadow. The largest ACE shows an amplitude of 5.4 °C and a 1% isotopic decline and is centred on ~14.0 ka BP, consistent with the timing of the GI-1d event in the Greenland stratigraphy. The two other observed ACEs are of smaller magnitude and are centred on ~13.6 ka BP and ~13.2 ka BP, with these smaller magnitude events tentatively correlated with the GI-1cii and GI-1b events, respectively, but lack sufficient chronological constraint to fully assess their timing. When comparing the Crudale Meadow record with other locations in the British Isles a strong relationship can be observed between the magnitude of T_{Jul} cooling and latitude, with a reduced signal in more southerly locations, indicating that oceanic forcing may be a key driver of the ACEs.

KEYWORDS: abrupt cooling event (ACE); British Isles; chironomids; GI-1d; stable isotopes

Introduction

The Last Glacial–Interglacial Transition (LGIT) (~16–8 ka BP) is characterised by a series of abrupt cooling events (ACEs) (Rasmussen *et al.*, 2006, 2014).

The most notable of these is the Greenland Stadial 1 (GS-1) (12 896–11 703 GICC05 b2k), recorded as the Younger Dryas in Europe and locally named the Loch Lomond Stadial (LLS) in Britain. This ACE occurs on a millennial scale and is widely preserved in a range of marine, ice-core and terrestrial archives (Lowe *et al.*, 2008). However, the LGIT is also punctuated by shorter-lived ACEs that operate on centennial timescales (Rasmussen *et al.*, 2014). Such events are clearly seen in the Greenland ice-core records during Greenland Interstadial 1 (GI-1) (14 692–12 896 GICC05 b2k), and also in the Windermere Interstadial (WI), the British correlative of GI-1, where at least three ACEs are recorded (e.g. Lang *et al.*, 2010; Brooks *et al.*, 2012). These centennial-scale ACEs are an important research priority as climate model simulations have demonstrated that northwest Europe will become increasingly susceptible to ACEs as greenhouse gas emissions increase (Gregory *et al.*, 2005; Petoukhov *et al.*, 2005; Hawkins *et al.*, 2011).

The structure and magnitude of these centennial-scale ACEs is poorly understood beyond the Greenland ice cores. This is because: (1) some proxies are insufficiently sensitive to record the full expression of these events (Lowe *et al.*, 1999); (2) many archives do not have sufficient sample resolution to reconstruct them in detail; and (3) some archives have insufficient stratigraphic resolution leading to a relatively poor expression in the sediment sequences of such short-lived climatic events. Even when the above are not an issue, the challenge of developing chronologies with the precision to accurately correlate centennial-scale climatic events has limited any discussions regarding climatic synchronicity (Björck *et al.*, 1998; Lowe *et al.*, 2008).

This study aims to investigate the spatial variations in the magnitude of WI ACEs across the British Isles, with a particular focus on the GI-1d cooling event. This paper presents new chironomid and $\delta^{18}O$ records from a lacustrine sediment sequence taken at Crudale Meadow, Orkney Isles, Scotland, improving the spatial coverage of temperature proxy records for the northerly reaches of the British Isles. Both chironomid and $\delta^{18}O$ analyses were applied at high resolution (approximately 20 years/sample resolution) allowing the nature of ACEs across this interval to be understood in greater detail than has been possible for most comparable records from northwest Europe. Both proxies are conducted on the same sequence (CRUM1) which ensures that samples are consistently taken from the same stratigraphic level. Furthermore, the site's robust independent chronology allows comparisons to be made with other archives such as the Greenland ice-core records, which also have $\delta^{18}O$ records with a resolution of approximately 20 years. The paper concludes with comparisons to a suite of other C-IT and $\delta^{18}O$ records from across the British Isles, discussing the regional and local variations in the magnitude of different ACEs within the WI.

Material and methods

Site description and previous work

Crudale Meadow (59°0′57.23″ N 3°19′42.72″ W; ~9 m a.s.l.) is a former lake basin situated on Mainland, the largest island of the Orkney archipelago (Fig. 1). The former lake covers an

*Correspondence: C. P. Francis, as above.
E-mail: Chris.francis@rhul.ac.uk

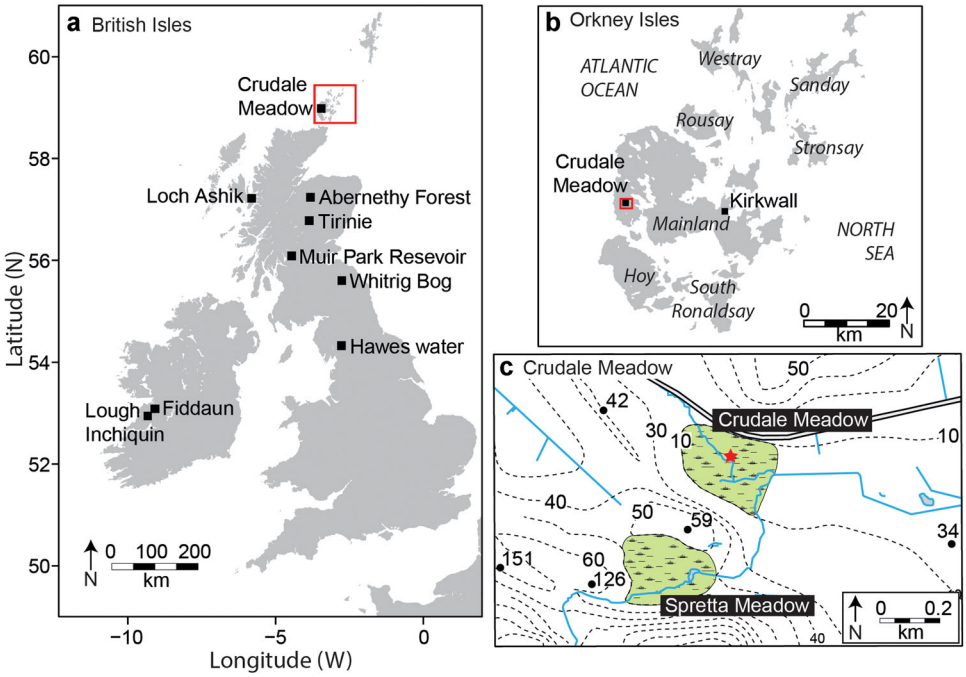

Figure 1. (a) A map of the British Isles and the position of Crudale Meadow in relation to other sites mentioned in the text which have chironomid-inferred temperatures (T_{Jul}) and/or oxygen isotope records ($\delta^{18}O$) covering the Windermere Interstadial (WI); (b) map of the Orkney Isles and position of Crudale Meadow on the west coast of Mainland; (c) Basin map of Crudale Meadow and its relation to neighbouring Spretta Meadow. Red star denotes core location. [Color figure can be viewed at wileyonlinelibrary.com]

area of approximately 0.09 km^2 and sits within a topographic depression between Devonian Qui Ayre sandstones and mid–late Devonian Upper Stromness Flagstones (Mykura *et al.*, 1976). Thin tills on the surrounding slopes are partially derived from the carbonate-rich dolomitic siltstones, shales and sandstones of the Middle Old Red Sandstone and Lower Stromness Flagstones (Whittington *et al.*, 2015). The in-filled lake basin currently contains a valley mire dominated by *Phragmites australis* and Cyperaceae and drains east via a small stream into the Loch of Stenness (Whittington *et al.*, 2015).

The Orkney archipelago currently has a cool–temperate climate and experiences mean daily maximum temperatures of 6.4 °C in January, 15.9 °C in July and 8 °C annually. These temperatures are relatively high when the latitude of the site is taken into consideration but can be explained by the warming influence of the North Atlantic current. Mean annual rainfall is 1038 mm with the majority of the precipitation falling in the winter months (data from the meteorological station at Kirkwall, 21 km east of Crudale Meadow; Met Office data 1981–2010). Further site details can be found in Whittington *et al.* (2015).

Previous studies obtained sediment records from the Crudale Meadow palaeolake with sequences composed of sediments dating to the WI, LLS and Holocene (Moar, 1969; Bunting, 1994; Whittington *et al.*, 2015), similar to numerous LGIT sequences from other parts of Scotland and the British Isles (Lowe and Walker, 1977; Lowe *et al.*, 1994). Whittington *et al.* (2015) identified three possible climate oscillations within sediments they believed to be of WI age. Attempts to construct an independent age model for the sequence using radiocarbon dates obtained from bulk sediments and aquatic remains yielded ages that were considered to be too old (Whittington *et al.*, 2015). Proposed correlations were made to the GI-1d, GI-1cii and GI-1b events based on stratigraphic alignment with the Greenland ice-core record, but a consequence of this approach means that the sequence of Whittington *et al.* (2015) lacks independent verification of the timings of the encountered events. Timms *et al.* (2018) retrieved a new sediment record from the same palaeolake (CRUM1), which also contained sediments of Dimlington age (*c.* Late GS-2; pre-14.7 ka BP). Timms *et al.* (2018) developed a tephrochronology and tephrostratigraphy for the LGIT, using 12 cryptotephra horizons and one visible tephra layer, producing one of the best age-constrained sequences in the British Isles for this period. While there are proxies for landscape stability derived from sediment parameters at this site, palaeoclimatic proxy data supported by an independent chronology are yet to be produced from the Timms *et al.* (2018) core.

Sedimentology and physical parameters

This study focuses on sediments identified as WI in age (602–645 cm depth) from the CRUM1 sequence recovered by Timms *et al.* (2018). Sediments were classified using Troels-Smith (1955) and colours identified using the Munsell Soil Colour system. Calcium carbonate ($CaCO_3$) content and the organic component of the sediments were determined using a Bascomb calcimeter (Gale and Hoare, 1991) and by loss-on-ignition (Heiri *et al.*, 2001), respectively. The present work has increased the $CaCO_3$ sampling resolution from 2 cm intervals as used in Timms *et al.* (2018) to contiguous 1 cm intervals across the WI and 0.5 cm intervals between 629 and 634 cm.

Chronology

The initial age–depth model for the sequence constructed by Timms *et al.* (2018) was based on the occurrence of 13 tephra layers, six of which correlated to known eruptions, and has been further improved with a single accelerator mass spectrometry radiocarbon date from the later part of the WI. The radiocarbon sample consisted of picked terrestrial plant macrofossil remains including leaves of *Dryas octopetala*, *Empetrum* and *Betula nana* along with fruits of *Betula nana* from between 614 and 615.5 cm. Analyses were performed at

Queen's University, Belfast. Our age–depth model was produced using the *P_Sequence* function as included in OxCal v 4.4.2 (Bronk Ramsey, 2008, 2009) and the IntCal20 calibration curve (Reimer *et al.*, 2020). The age estimates for the Borrobol, Penifiler and Vedde Ash tephra layers are based on remodelling of the data presented in Kearney *et al.* (2018) utilising the IntCal20 curve and are identical to those report by Timms *et al.* (in press). All interpolated dates are rounded to the nearest decade to avoid spurious precision and are accompanied by 1σ errors.

Chironomid analysis

The sequence was sampled at 0.5 cm resolution for chironomids between 649 and 597 cm depth where every second sample was analysed for chironomids. Samples were contiguously analysed in intervals where preliminary data revealed notable changes. The sediment properties of the marl meant the standard laboratory approach outlined in Brooks *et al.* (2007) was not effective in releasing the chironomid head capsules in a clean identifiable state. We experimented with a range of additional laboratory procedures to improve head capsule recovery (see Supplementary information 1). Our final laboratory protocol starts by disaggregating sediment in 10% KOH for 20 min at 75 °C followed by sieving over 90 and 212 µm meshes. This initial stage was followed by submerging the samples in a sonic bath for between 2 and 5 s, followed by a second phase of sieving to remove the newly disaggregated marl. The use of the sonic bath increased head capsule yield by up to 300%. The residue was then transferred to a Bogorov sorting tray and chironomid head capsules (HCs) were handpicked from the residue using fine forceps under a Motic SMZ-168-BP stereo microscope at 25× magnification and mounted on permanent microscope slides using Hydromatrix mounting medium. Chironomid HCs were identified using a binocular CX41 microscope at 400× magnification in accordance with Brooks *et al.* (2007), Rieradevall and Brooks (2001) and Wiederholm (1983).

Several samples with low count sums were amalgamated with adjacent samples with the aim of reaching a minimum count sum of 50 HCs per sample (e.g. Heiri and Lotter, 2001; Quinlan and Smol, 2001). This resulted in a dataset with 63 fossil samples, of which four samples did not reach the minimum count sum of 50 HCs even after sample amalgamation (samples at 649, 648, 647 and 597 cm; count sum range 39–48 HCs). However, as these samples had a low variety of taxa present, we chose to retain these samples in subsequent numerical analyses, assuming that the count sums of 40–50 are sufficient to provide reliable estimates of past temperatures (Quinlan and Smol, 2001). A percentage diagram was constructed using C2 version 1.7.7 (Juggins, 2007). Zonation of the chironomid diagram was derived using the CONISS clustering algorithm (Grimm, 1987) where statistical significance of the zones was determined using a Broken Stick model (Bennett, 1996). Zonation analyses were conducted in R (R Core Team, 2018) using the vegan (Oksanen *et al.*, 2017) and rioja (Juggins, 2017) packages.

The 274-lake combined Swiss–Norwegian chironomid–climate calibration dataset was used to estimate July air temperatures (T_{Jul}; Heiri *et al.*, 2011). This calibration dataset has several advantages over the Norwegian dataset (Brooks and Birks unpublished; see Supplementary information 2) which is more commonly applied to British lake records (e.g. Brooks *et al.*, 2012, 2016): it contains a higher number of taxa, it covers a larger temperature gradient, and it incorporates alkaline carbonate lakes with a chemistry similar to that which is supposed to have been present at Crudale Meadow during the WI.

Head capsule preservation in our fossil samples was generally good, allowing identification to a high taxonomic resolution. However, some taxa had to be combined in both the fossil samples as well as in the calibration dataset in order to allow numerical comparisons. *Paratanytarsus austriacus*-type and *Paratanytarsus penicillatus*-type were combined to *Paratanytarsus* undifferentiated due to the low number of mandibles preserved attached to HCs (*c.* <10%), prohibiting the differentiation of these morphotypes with any degree of confidence. *Corynocera oliveri*-type and *Tanytarsus lugens*-type were combined and are referred to as *COTL*-type, as they were hard to distinguish due to the varying degree of overlap between the lateral teeth on the mentum.

A two-component weighted averaging partial least squares (WA-PLS; ter Braak and Juggins, 1993; ter Braak *et al.*, 1993) regression model was selected for reconstruction purposes as it combines the best predictive power with a root mean squared error of prediction of 1.4 °C, r^2_{jack} of 0.9 °C and maximum $bias_{jack}$ of 0.9 °C, as estimated using leave-one-out cross-validation. Sample-specific errors for our reconstructed T_{Jul} values were calculated by 999 bootstrap cycles. The chironomid percentage data were square-root transformed prior to analysis to minimise variances, and 19 outlier lakes were removed prior to analysis. T_{Jul} and sample-specific errors were calculated in C2 (Juggins, 2007). A reconstruction based on the Norwegian calibration dataset is provided for comparison in the Supplementary information.

Several methods were used to test the reliability of the chironomid-based temperature reconstruction (Birks *et al.*, 1990; Engels *et al.*, 2010). The percentage abundance of the identified subfossil chironomids that are absent from or rare in the calibration dataset was calculated for each fossil sample. A taxon was considered rare if it had a Hill's N2 (Hill, 1973) below 5 in the calibration dataset (Birks *et al.*, 1990). Modern analogue technique (MAT) analysis was performed to assess the similarity of fossil assemblages to those in the modern calibration dataset. Cut-levels of the 5th and 10th percentiles of all squared-chord distances in the modern calibration data were used to determine 'no close' and 'no good' analogues and were compared with the distance between an individual subfossil assemblage and its nearest modern analogue (Telford, 2014a). MAT analysis was conducted in R using the analogue package (Simpson, 2020) with squared-chord distance used as a measure of dissimilarity. Samples were not square-root transformed prior to analysis. A goodness-of-fit test was performed using canonical correspondence analysis (CCA) (ter Braak, 1986) with July air temperature as the sole constraining parameter with the subfossil samples added passively in the analysis. Residual distances of the subfossil samples to the first CCA axis were compared with the residual distances of all the modern samples to the first CCA axis. Thresholds of the 90th and 95th percentile of residual distances of modern calibration dataset samples to CCA axis 1 were used to identify subfossil samples with a 'poor' or 'very poor' fit with temperature (Telford, 2014b). CCA analysis was conducted in R using the vegan package (Oksanen *et al.*, 2017). Samples were not square root transformed prior to these analyses.

Stable isotope analysis

Samples for stable isotope analysis ($\delta^{18}O$ and $\delta^{13}C$) were taken at 0.5 cm intervals. Approximately 0.5 cm^3 of sediment was disaggregated in sodium hexametaphosphate ($(NaPO_3)_6$) overnight, then sieved through a 63 µm nylon mesh. This removed any shell fragments from ostracods and molluscs, which are known to strongly fractionate oxygen isotopes and can

therefore adversely affect the isotopic signal of the autogenic calcite lake sediments (Candy *et al.*, 2016). The <63 µm fraction, largely autogenic calcite precipitated from the water column, was retained and treated with hydrogen peroxide (H_2O_2) to remove other organic material. Samples were then air-dried and weighed using a Mettler Toledo XP6 microbalance. Samples were digested in phosphoric acid at a temperature of 90 °C to produce CO_2 from which the $\delta^{18}O$ and $\delta^{13}C$ were then analysed using a ThermoFisher Delta Plus XP mass spectrometer with a Gasbench II preparation system. Three internal standards (BDH) were analysed every five samples and three external standards (NBS-19) were analysed in each machine run. Internal precision produces analytical uncertainties of ±0.07 ($\delta^{18}O$) and ±0.04 ($\delta^{13}C$).

Results and interpretation

Sedimentology and chronology

The CRUM1 palaeolake sequence consists of an alternation between two marl units and two minerogenic units (Timms *et al.*, 2018; Fig. 2a). Here we focus on units CM-L1 to -L3 (Fig. 2b; Table 1). The lowermost unit (CM-L3) is composed of silts and clays ($CaCO_3$ ~10%) and is succeeded by a marl unit (CM-L2), which is subdivided into eight subunits (Fig. 2b; Table 1). The $CaCO_3$ content increases in CM-L2a from ~20% to ~70% in CM-L2b and remains at this level for the remainder of CM-L2. However, subunits within CM-L2 show falls in $CaCO_3$ from 67% to 8% (632 cm; CM-L2c) and smaller decreases in $CaCO_3$ to 60% and 65% in CM-L2e (~620 cm) and CM-L2g (~610 cm), respectively. These decreases in percentage $CaCO_3$ are normally accompanied by an increase in minerogenic material, rather than an increase in organic content (Fig. 2b). Leaves of *Dryas octopetala*, *Empetrum* and *Betula nana*, along with fruits of *Betula nana*, were found infrequently throughout CM-L2d to CM-L2h. Unit 3 is predominantly silty clay with little or no $CaCO_3$, but higher organic content is present in CM-L3a (~10%) before this decrease that occurs within CM-L3b.

The silty clay deposition at the base of the sequence shows high levels of mineral in-wash to the basin from the lake catchment. This often indicates relatively low biogenic productivity and enhanced erosion of soils into streams during high discharge events (Palmer *et al.*, 2015; Candy *et al.*, 2016). The change to a system dominated by marl sedimentation is indicative of higher biological activity within the lake and its catchment that allows precipitation of calcite crystals within the lake. Calcite production may also be enhanced by a decrease in the mineral sediment load transported to the basin due to increased plant growth in the catchment stabilising the soil (Palmer *et al.*, 2015; Candy *et al.*, 2016). The transition between mineral-rich sedimentation and marl sedimentation may, therefore, relate to a climatically induced change impacting the lake sedimentation. The lower silty clays are thought to reflect deposition during the colder climatic conditions of the Dimlington Stadial (DS; CM-L1) and the marl sedimentation to reflect warmer climatic conditions of the WI (CM-L2), before the return to colder climatic conditions of the LLS represented by CM-L3. More subtle lithological variability is also recorded within CM-L2 which will be explored further in this paper.

This interpretation is supported by the independent age model for CRUM1 (Timms *et al.*, 2018). The marl unit (CM-L2) represents the WI due to the presence of the Borrobol Tephra at 638 cm (14 107 ± 58 cal a BP) and the Penifiler Tephra at 632 cm (14 024 ± 77 cal a BP). The presence of the Vedde Ash at 587 cm (11 997 ± 39 cal a BP) in the following minerogenic unit (CM-L3) means these sediments were deposited during the LLS. The additional radiocarbon sample yielded an uncalibrated age of 11 626 ± 53 ^{14}C a BP, and a calibrated modelled age of 13 491 ± 67 cal a BP, providing further confirmation of the WI age of CM-L2. The radiocarbon date has reduced the age error estimate for the mid-WI by more than 50%.

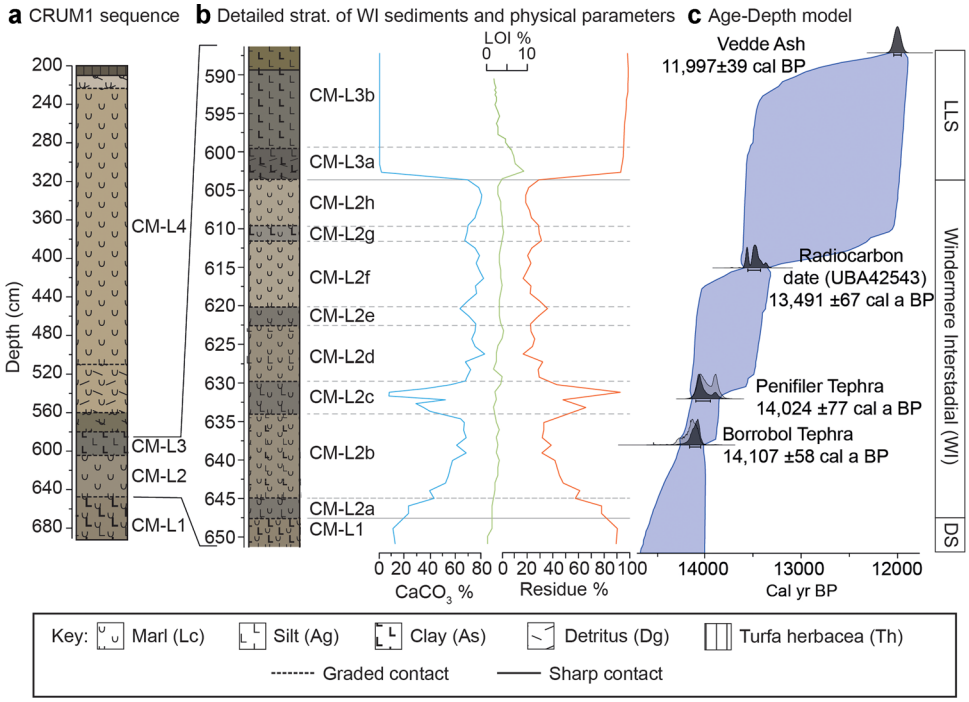

Figure 2. Sedimentological, isotopic and chronological data from the CRUM1 sequence. (a) Simplified lithostratigraphy of the CRUM1 sequence at Crudale Meadow, spanning the Lateglacial and Early Holocene; (b) detailed lithostratigraphy of the WI and early Loch Lomond Stadial showing proportions (%) of calcium carbonate ($CaCO_3$), organic (loss-on-ignition) and minerogenic components. Lithostratigraphic zones are labelled CM-Ln and colours are from the Munsell colour system; (c) Age–depth model with additional radiocarbon date (UBA42543). The raw uncalibrated age of the radiocarbon date is 11 626 ± 53 ^{14}C a BP. [Color figure can be viewed at wileyonlinelibrary.com]

Table 1. Lithostratigraphic units in the CRUM1 sequence mentioned in the text

Unit	Depth (cm)	General description	Troels-smith	Munsell colour
CM-L3b	≤599	Silty clay	As2 Ag2	5Y 4/1 dark grey
CM-L3a	599–602	Silty clay with organic detritus	As2 Ag1 Dg1	2.5Y 3/1 very dark grey
CM-L2h	602–609	Marl	Lc4	5Y 5/1 grey
CM-L2g	609–611	Silty clay Marl	Lc2 Ag1 As1	5Y 4/1 dark grey
CM-L2f	611–620	Marl	Lc4	5Y 5/1 grey
CM-L2e	620–622	Silty marl	Lc2 Ag2	2.5Y 4/1 dark grey
CM-L2d	622–630	Silty marl	Lc2 Ag2	5Y 5/1 grey
CM-L2c	630–634	Silty clay marl	Ag2 As1 Lc1	5Y 4/1 dark grey
CM-L2b	634–645	Silty clay marl	Lc2 Ag1, As1	5Y 5/1 grey
CM-L2a	645–648	Silty marl	Ag2 Lc2	5Y 4/1 dark grey
CM-L1	≥648	Silty clay, some carbonate	Ag2 As1 Lc1	5Yr 4/1 dark grey

Chironomids

Chironomid assemblages

In total, 51 different chironomid taxa were identified in the 63 samples analysed, with assemblages displaying considerable down-core variation (Fig. 3). Head capsule concentrations are generally high throughout the sequence, except in CM-C1 and CM-C6, where there are less than 30 HCs/g. The majority of taxa present at Crudale Meadow are lacustrine in nature and as most chironomid taxa are indicative of intermediate water depths we suggest that a moderately deep lake (approximately 5–7 m deep) was present at the site throughout the LGIT (Engels and Cwynar, 2011).

Six statistically significant assemblage zones were identified. The basal unit, CM-C1 (650–646.5 cm; pre-14,180 ± 150 cal a BP) is dominated by cold-stenothermic taxa typically found in the profundal of oligotrophic lakes (e.g. *COTL*-type, *Monodiamesa*; Brundin, 1956; Kansanen, 1985; Brodin, 1986).

The onset of CM-C2 (646.5–633.75 cm; 14 180 ± 150 to 14 050 ± 80 cal a BP) shows a decline in ultra-cold and cold-indicating taxa, to nearly 0%, while cool–temperate and temperate taxa increase in abundance to over 95%. The chironomid fauna of CM-C2 are dominated by taxa which indicate well-oxygenated mesotrophic conditions, e.g. *Psectrocladius sordidellus*-type (Moller Pillot, 2013), *Procladius* (Brodin and Gransberg, 1993) and *Tanytarsus pallidicornis*-type (Brodin, 1986). There is a large increase in the range of taxa present from CM-C1 to CM-C2, which typically occurs under warmer conditions (Engels *et al.*, 2020). The presence of *Dicrotendipes nervosus*-type and *Ablabesmyia* suggests the development of aquatic macrophytes in the lake (Brodersen *et al.*, 2001; Vallenduuk and Moller Pillot, 2007; Moller Pillot, 2009).

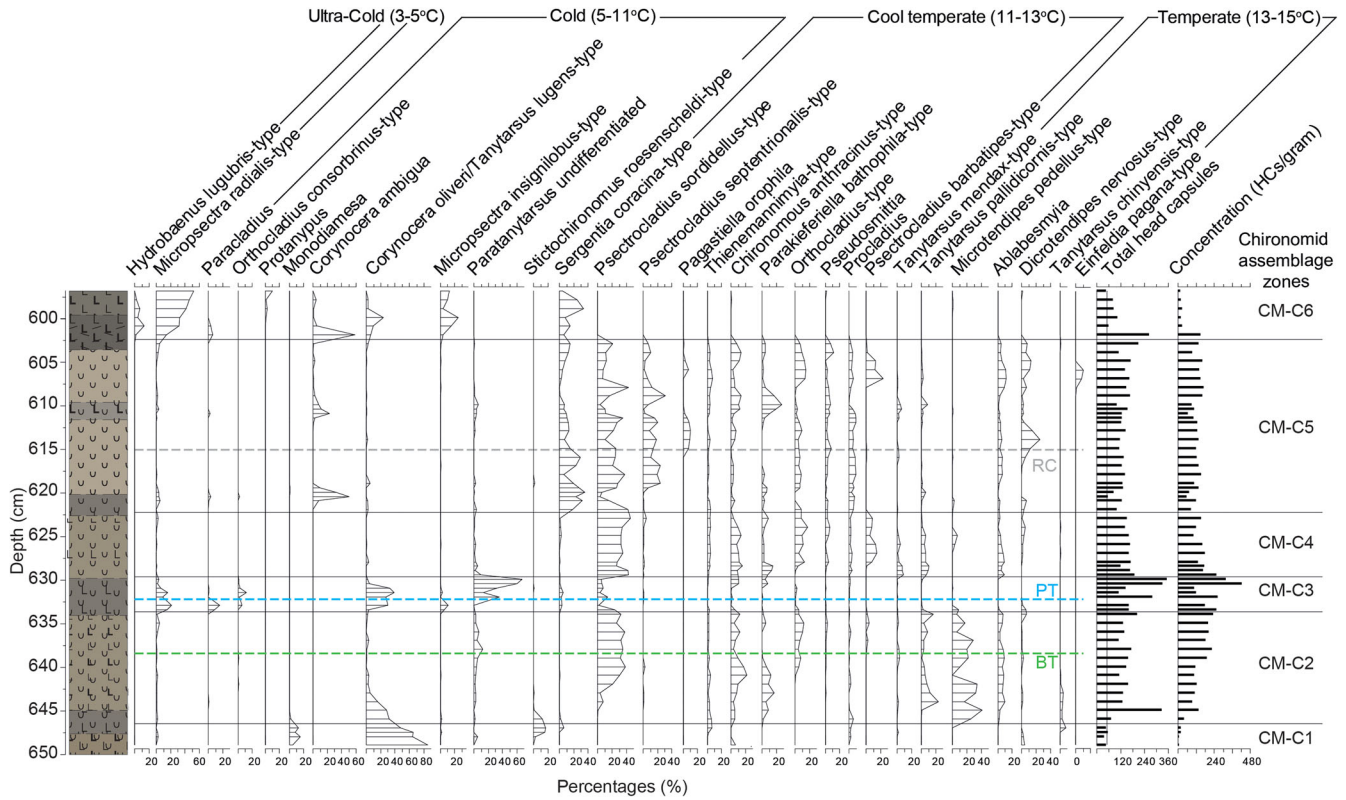

Figure 3. Percentage abundance diagram of selected chironomid taxa present in the Windermere Interstadial (WI) sediments at Crudale Meadow alongside the CRUM1 sequence stratigraphy. The positions of the Borrobol Tephra (BT; 14 107 ± 58 cal a BP) and Penifiler Tephra (PT; 14 024 ± 77 cal a BP) are denoted by the green and blue dashed lines, respectively. The position of the radiocarbon date (RC) is marked by the grey dashed line and has an age of 13 491 ± 67 cal a BP. Chironomid assemblage zones are marked on the right. Taxa are arranged by their T_{Jul} optima in the modern calibration dataset (Heiri *et al.*, 2011) as calculated using a weighted-averaging model with coolest optima on the left and warmest optima on the right. Head capsule concentrations (HCs/g) and total head capsule counts are displayed on the right. [Color figure can be viewed at wileyonlinelibrary.com]

The abrupt increase in *Microtendipes pedellus*-type to 4% at the onset of CM-C2 suggests relatively warm mesotrophic conditions were established very early on in the WI (Brooks *et al.*, 2012).

A centennial-scale cooling event occurs during CM-C3 (633.75–629.75 cm; 14 050 ± 80 to 13 960 ± 160 cal a BP) where assemblages revert to a fauna dominated by cold-stenothermic taxa typical of oligotrophic lakes. Temperate taxa associated with mesotrophic conditions and macrophytes virtually all disappear from the assemblage (e.g. *D. nervosus*-type and *Ablabesmyia*) during CM-C3, while only a few cool–temperate taxa persist in very low numbers (e.g. *P. sordidellus*-type). The presence of *Paratanytarsus* suggests aquatic macrophytes may still be present in the lake (Brooks *et al.*, 2007). *Paracladius* indicates the input of organic detritus which it can exclusively feed on (Moller Pillot, 2013).

CM-C4 (629.75–622.75 cm; 13 960 ± 160 to 13 730 ± 210 cal a BP) has a similar assemblage composition to CM-C2, with *P. sordidellus*-type, *Chironomous anthracinus*-type and *Orthocladius*-type indicating warm mesotrophic conditions. *D. nervosus*-type and *Ablabesmyia* re-establish, suggesting aquatic macrophytes proliferate again (Brodersen *et al.*, 2001; Vallenduuk and Moller Pillot, 2007; Moller Pillot, 2009). However, *M. pedellus*-type virtually disappears during CM-C4, possibly as a result of more stable conditions (Brooks *et al.*, 2007).

Warm conditions continue into CM-C5 (622.75–602.5 cm; 13 730 ± 210 to 12 830 ± 520 cal a BP). However, the notable increase in *S. coracina*-type, a cold-stenothermic taxon (Brodin, 1986), to an average of 15% suggests marginally cooler conditions during the latter part of the WI. The low abundance but persistent presence of *Pseudosmittia* at ~3% in CM-C5 may indicate enhanced stream input and/or erosion of the landscape as the species within this genus are typically terrestrial or semi-terrestrial (Cranston, 1982; Massaferro and Brooks, 2002). Two minor reorganisations in the chironomid fauna occur during CM-C5 at 622–617 cm (13 710 ± 210 to 13 550 ± 150 cal a BP) and 612–608 cm (13 330 ± 320 to 13 120 ± 450 cal a BP) with *Corynocera ambigua* increasing markedly to 31% and 14%, respectively. *C. ambigua* thrives in cold, unstable, transitional environments (Brodersen and Lindegaard, 1999). A change in the composition of aquatic macrophytes may also be partially responsible as *C. ambigua* is often associated with charophytes (Brodersen and Lindegaard, 1999). Chara oospores were encountered during HC picking at depths where *C. ambigua* increased in abundance. Other cold-stenothermic taxa also show minor increases at 622–617 cm and 612–608 cm, including *M. radialis*-type, *Paracladius and Orthocladius consorbrinus*-type. Concurrent declines in taxa adapted to warmer conditions also occur in *P. sordidellus*-type, *P. septentrionalis*-type and *D. nervosus*-type.

A notable change in taxa occurs at the onset of CM-C6 (602.5–595 cm; 12 830 ± 520 to 12 430 ± 470 cal a BP). A return to very cold oligotrophic conditions is indicated by the dominance of cold stenotherms, e.g. *Micropsectra insignilobus*-type (Brundin, 1956), *Hydrobaenus lugubris*-type (Cranston *et al.*, 1983) and *Protanypus* (Moller Pillot, 2013) contributing up to 25%, 13% and 10%, respectively. Conditions may have been ultra-oligotrophic as inferred from the dominance of *M. radialis*-type (Brodin, 1986), which forms up to 52% of the assemblages. Another discrete peak of 58% in *C. ambigua* occurs at the start of this zone indicating another period of instability (Brodersen and Lindegaard, 1999).

Chironomid-inferred July temperature reconstruction

The chironomid-inferred mean July air temperatures record (T_{Jul}) (Fig. 4) shows a rapid increase from 7.5 ± 1.5 °C in CM-C1 to 11.5 ± 1.4 °C early in CM-C2. T_{Jul} continues to increase

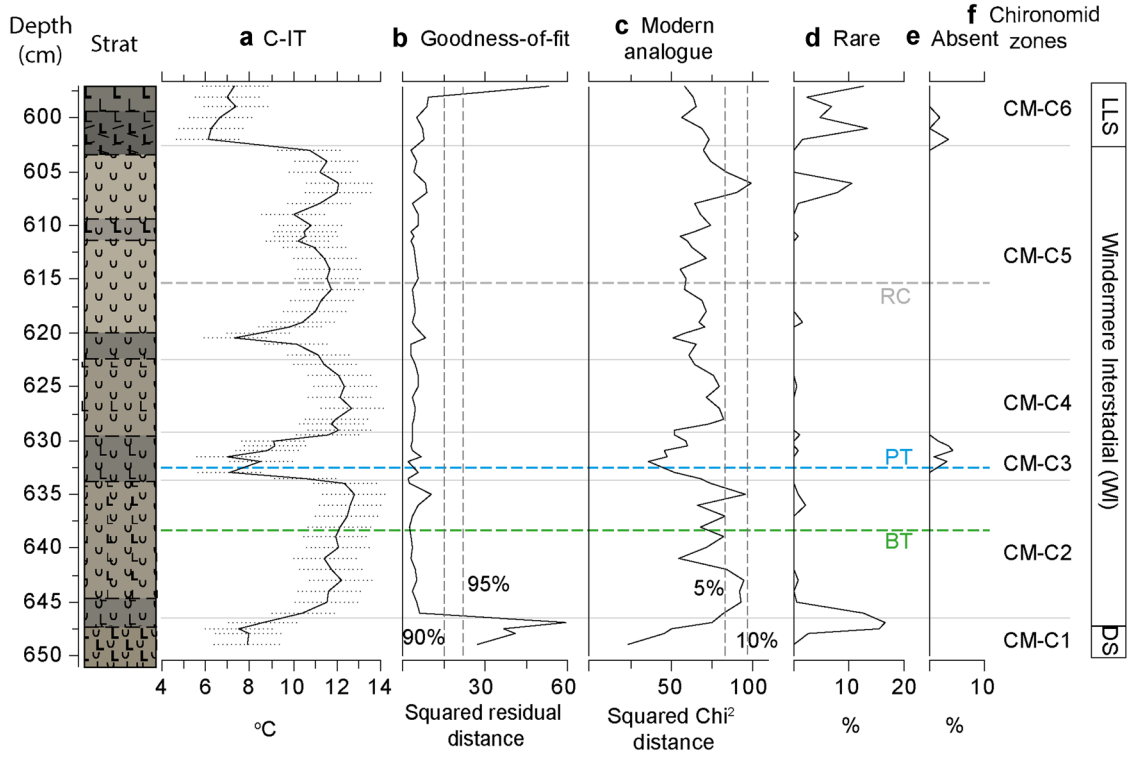

Figure 4. (a) Chironomid-inferred mean July air temperature estimates with sample-specific error bars; (b) Goodness-of-fit of the fossil assemblages to temperature, with dashed lines representing the 90th and 95th percentile of squared residual distance of modern samples to the first axis of a CCA; (c) Distance to the nearest modern analogue with dashed lines showing the 5th and 10th percentile of the Chi^2 distances of all samples in the modern calibration dataset; (d) Abundance of fossil taxa present in the down-core record which are rare in the modern calibration dataset, defined by Hill's N2 < 5; (e) Abundance of fossil taxa not present in the modern calibration dataset; (f) Chironomid assemblage zones. The Borrobol Tephra (14 107 ± 58 cal a BP) is marked in green and the Penifiler Tephra (14 024 ± 77 cal a BP) in blue. [Color figure can be viewed at wileyonlinelibrary.com]

throughout CM-C2, albeit more slowly, reaching a maximum of 12.8 ± 1.4 °C. A strong decline of 5.4 °C occurs during CM-C3, with T_{Jul} decreasing to 7 ± 1.4 °C, but recovers to 12.7 ± 1.4 °C in CM-C4. During CM-C5, two smaller declines in T_{Jul} occur, decreasing to 7.3 ± 1.4 °C at 620.5 cm and 10 ± 1.4 °C at 609 cm, a decline of 3.9 °C and 1 °C, respectively. Between CM-C5 and CM-C6 there is a large decline of 5 °C with T_{Jul} falling to 6.1 ± 1.5 °C. Sample specific errors range between 1.41 °C and 1.59 °C.

All samples of WI age have a good fit-to-temperature suggesting T_{Jul} is the major driver in chironomid assemblage change (Fig. 4b). It is noted that samples in LLS (CM-C6) and DS (CM-C1) generally have a 'very poor' fit-to-temperature. However, the discussion of the results for the stadial samples is beyond the aim and scope of this paper. The fossil assemblages also generally compare well to those in the modern calibration dataset, with 55 samples having good modern analogues (Fig. 4c). Although Seven samples had 'poor' modern analogues and one 'very poor' analogues in the modern calibration dataset, WA-PLS can still perform very well in non-analogous situations (Birks, 1998). The vast majority of taxa that occur during the LGIT at Crudale Meadow are well represented in the modern calibration dataset (Fig. 4d and e). Taxa that are rare in the modern dataset (i.e. Hills N2 < 5) remain very low throughout most of the WI, reaching a maximum of 2.2%, and are therefore unlikely to adversely influence the reconstruction. The only taxon not present in the modern calibration dataset is *Propsilocerus lacustris*-type, but this taxon does not exceed 4.1% in the five samples in which it occurs during CM-C3 (Fig. 4e).

Stable isotopes

For much of the WI the $\delta^{18}O_{Carbonate}$ values remain relatively stable throughout, oscillating around an average of −4.6% (1σ = 0.3%) (Fig. 5). The exceptions to this are: (1) a number of short-lived falls in $\delta^{18}O_{Carbonate}$ values (CM-O3, CM-O4b and 4d and CM-06); and (2) uniquely high $\delta^{18}O_{Carbonate}$ values of ~−2% in CM-O1, 2.5% higher than any other values in the dataset. The greatest decline in isotope values occurs during CM-O3, where $\delta^{18}O_{Carbonate}$ decreases from −4.6% to −5.6% at 632 cm, an isotopic shift to more negative values by 1%. Smaller isotopic declines are present in the remainder of the WI with a 0.4% shift to −5% during CM-O4b, a 0.7% shift to −5.3% in CM-O4d and a 0.5% shift to −5.1% in CM-O6. No carbonate was present in CM-L3 and so no bulk isotope data are available for this section of the sequence. The $\delta^{18}O$ signal of lacustrine carbonate ($\delta^{18}O_{Carbonate}$) sequences in the Lateglacial of northwest Europe is frequently interpreted as a palaeotemperature proxy (e.g. Diefendorf *et al.*, 2006; Van Asch *et al.*, 2012). The rationale for this is that $\delta^{18}O_{Carbonate}$ is controlled by the $\delta^{18}O$ of the lake water ($\delta^{18}O_{lake\ water}$) and the temperature at which the carbonate is precipitated in the water column (Talbot 1990; Leng and Marshal, 2004). In turn, $\delta^{18}O_{lake\ water}$ is largely a function of the $\delta^{18}O$ of rainfall ($\delta^{18}O_{precipitation}$) which is primarily controlled by the prevailing air temperature with other factors also having a small influence (Rozanski *et al.*, 1992, 1993). Such other factors include the amount, effect, water vapour source, seasonality of rainfall, or the distance of air masses from moisture source (Rozanski *et al.*, 1992, 1993). However, it is often assumed that none of these other factors exerts as strong an influence as air temperature on the $\delta^{18}O_{Carbonate}$ of lacustrine sequence in the Lateglacial in Britain. This can be seen in many Lateglacial sequences, such as that of Hawes Water (Marshall *et al.*, 2002) and Fiddaun (Van Asch *et al.*, 2012) which shows high $\delta^{18}O_{Carbonate}$ values in the warm early Holocene and WI but low values in the cold LLS.

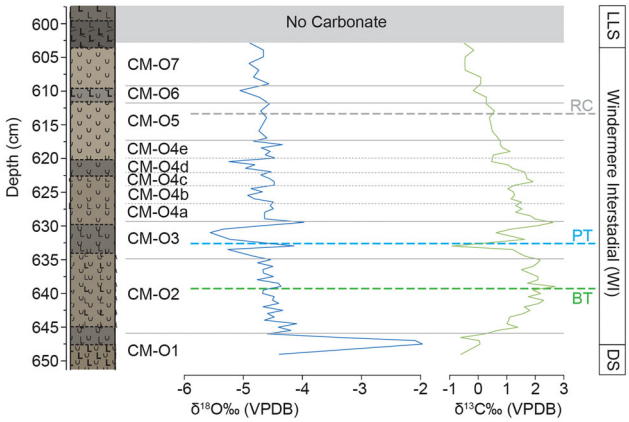

Figure 5. Stable isotope data ($\delta^{18}O$ and $\delta^{13}C$) for the Windermere Interstadial with zones denoted as CM-O*n*. [Color figure can be viewed at wileyonlinelibrary.com]

The $\delta^{13}C_{Carbonate}$ record from Crudale displays a rapid rise from −0.2% in CM-O1 to 2.7% in CM-O2. During CM-O3 $\delta^{13}C_{Carbonate}$ briefly declines to -0.9% but recovers to 2.6% by the end of the zone. Throughout CM-O4, −O5 and −O6, $\delta^{13}C_{Carbonate}$ steadily declines from 2.6% to -0.8%. The $\delta^{13}C$ of lacustrine carbonates ($\delta^{13}C_{Carbonate}$) is largely controlled by the dissolved inorganic carbon (DIC) of lake waters. DIC is influenced primarily by the carbon isotopic composition of the ground and surface waters recharging the lake, biological activity in the lake basin and the equilibration of CO_2 between the lake water and atmosphere (Leng and Marshall, 2004; Candy *et al.*, 2016). Therefore, $\delta^{13}C_{Carbonate}$ records a much more local signal than $\delta^{18}O$. Many $\delta^{13}C_{Carbonate}$ records from British carbonate sequences exhibit a gradual decline throughout the WI (e.g. Diefendorf *et al.*, 2006; Van Asch *et al.*, 2012; Candy *et al.*, 2016) caused by landscape revegetation following the DS (see Candy *et al.*, 2016 for discussion).

As with the studies outlined above, we also assume that palaeotemperature is the primary control on the $\delta^{18}O_{Carbonate}$ signal of the CRUM1 sequence. There is negligible evidence for other factors that may control the $\delta^{18}O_{Carbonate}$ signal; in particular, evaporation and detrital contamination, which are discussed further in the following paragraphs.

Lakes that are strongly influenced by evaporation may not preserve temperature trends clearly within the $\delta^{18}O_{Carbonate}$ record. This is because the $\delta^{18}O_{water}$ may be increased due to evaporation prior to carbonate precipitation, disrupting the relationship between air temperature and $\delta^{18}O_{water}$ (Leng and Marshall, 2004). In such systems there is often a strong relationship between $\delta^{18}O_{Carbonate}$ and $\delta^{13}C_{Carbonate}$ as the effect of increasing evaporation is to cause both of these to increase (Talbot, 1990). There is no covariance between $\delta^{18}O_{Carbonate}$ and $\delta^{13}C_{Carbonate}$ in the CRUM1 sequence, suggesting that evaporation did not exert a strong influence on the isotopic record at this site (Fig. 6). Furthermore, the $\delta^{13}C_{carbonate}$ of lake environments is typically between −3 and +3% in an open system (Talbot, 1990) and the values of −0.9 to +2.7% observed for our Crudale Meadow record fall within this range.

In sequences that are dominated by authigenic carbonate, such as CM-L2 with ~65% carbonate, the effect of detrital contamination is likely to be minimal because any in-washed fragments of bedrock would have been so heavily diluted by authigenic calcite precipitation that it would not impact the overall $\delta^{18}O_{Carbonate}$ value. However, in parts of a sequence where authigenic carbonate is low, i.e. CM-O1 and CM-O3, the presence of in-washed limestone particles may strongly

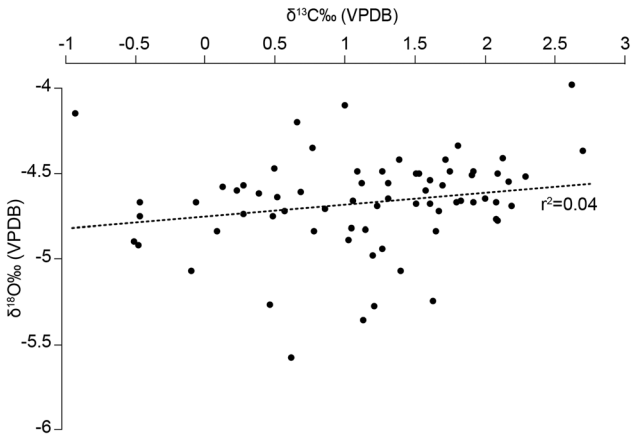

Figure 6. Comparison of $\delta^{18}O_{Carbonate}$ and $\delta^{13}C_{Carbonate}$ values showing an r^2 coefficient of 0.04. The samples from CM-O1 have been removed from the biplot as they are likely affected by detrital contamination.

influence both the $\delta^{18}O_{Carbonate}$ and $\delta^{13}C_{Carbonate}$ values. This is clearly seen in CM-01 where low percentage $CaCO_3$ values are associated with uniquely high $\delta^{18}O_{Carbonate}$ values. However, this contrasts with CM-O3, where an interval of low percentage $CaCO_3$ values is associated with the lowest $\delta^{18}O_{Carbonate}$ values in the sequence. These low isotopic values are likely to primarily record the $\delta^{18}O_{Carbonate}$ of authigenic carbonate, as detrital contamination would result in higher $\delta^{18}O_{Carbonate}$ values. Some contamination of the $\delta^{18}O_{Carbonate}$ could exist, with the effect of masking the true values in this interval, but it is likely that the $\delta^{18}O_{Carbonate}$ values of CM-O3 are mostly controlled by the $\delta^{18}O_{Carbonate}$ of authigenic carbonate.

Our $\delta^{18}O$ record broadly corresponds with that of $\delta^{18}O$ record previously published by Whittington *et al.* (2015) in terms of the number and structure of events, although there is less variance in our $\delta^{18}O$ data. This is potentially due to the differing sample preparation methods used between this study and Whittington *et al.* (2015), where the latter dry-sieved samples at 100 µm to remove detrital fragments. Despite similarities between the two isotope records, the lack of independent chronological control within the Whittington *et al.* (2015) data means it is difficult to make robust comparisons between the two datasets.

Discussion

Synthesis: temperature reconstructions at Crudale Meadow

The Crudale Meadow chironomid-inferred temperature record (T_{Jul}) and oxygen isotope record ($\delta^{18}O$) provide independent indicators of summer and annual temperature variability, respectively, across the WI. Overall, there is good agreement between both proxies, broadly showing three centennial-scale cooling events separated by four warm intervals (Fig. 7). While chironomid-based climate reconstructions provide quantified July temperature estimates, quantified temperature values cannot be produced from the $\delta^{18}O$ record. This is because temperature is only one of the factors that controls this proxy.

It should be noted that there are short-lived declines in $\delta^{18}O_{Carbonate}$ values that have either no or negligible expression in the T_{Jul} record, i.e. CM-O4b. This does not mean that these are not climatic events but could simply reflect that, at times, the $\delta^{18}O_{Carbonate}$ and the T_{Jul} are recording different parts of the climate system. Although lake carbonates precipitate primarily in the late spring/early summer, they are precipitating from lake waters that frequently reflect the $\delta^{18}O$ of groundwater which is in turn composed of homogenised rainfall from across the year (Blockley *et al.*, 2018). Also, small–medium sized open lake systems with shifts in $\delta^{18}O$ of a few permillage points, such as the Crudale Meadow palaeolake, often have residence time of ≥1 yr (Leng and Marshall, 2004). This means that the $\delta^{18}O_{Carbonate}$ value reflects an approximate average of the $\delta^{18}O$ value of annual rainfall and, therefore, an approximate average of annual air temperatures. The chironomid-based reconstruction, as outlined above, records July temperatures. Consequently, if an ACE occurs and winter temperatures decline but summer temperatures are relatively unaffected, the ACE may have an expression in the $\delta^{18}O_{Carbonate}$ values but not in T_{Jul} (Blockley *et al.*, 2018). It is, therefore, likely that some of the climatic events seen in the CRUM1 record affect winter temperatures more strongly than summer temperatures. Here we examine the magnitude and timing of the observed temperature reconstructions at Crudale Meadow. To help synthesis the proxy data, a number of climate zones have been formed and are denoted as CM-CZn.

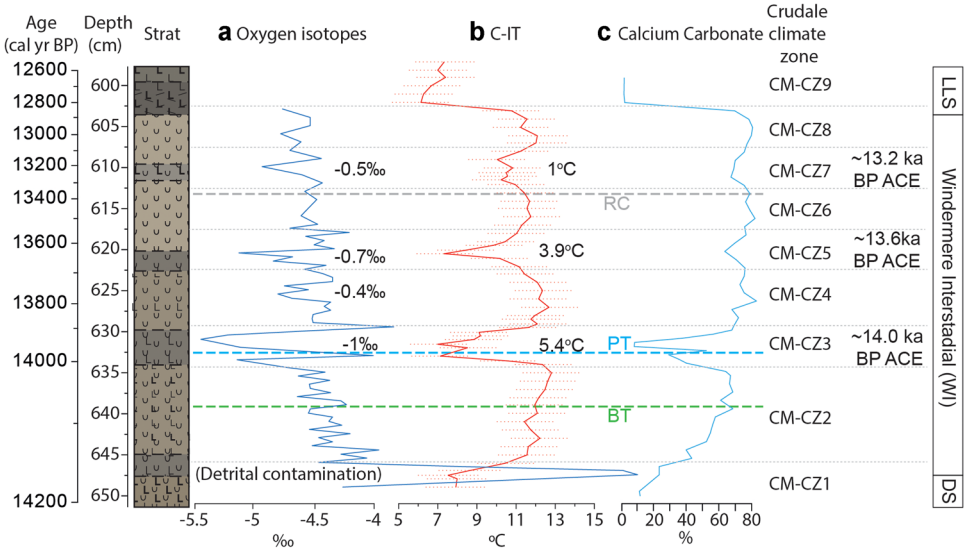

Figure 7. Comparison diagram of the main proxies at Crudale Meadow. (a) Oxygen isotopes; (b) Chironomid-inferred mean July air temperatures (T_{Jul}); (c) Calcium carbonate. The sequence has been split into a number of climate zones (CM-CZ*n*). [Color figure can be viewed at wileyonlinelibrary.com]

Dimlington Stadial and Windermere Interstadial onset (CM-CZ1 and -CZ2) ~14 180 ± 150 cal a BP

The lowermost zone, CM-CZ1, is characterised by a very cold climate with T_{Jul} ~8 °C, dominated by minerogenic deposits and dated to the DS (Fig. 8). The $\delta^{18}O$ values of approximately −2% are outliers in this record caused by detrital contamination from geological carbonate. Crudale Meadow represents only the second chironomid-based temperature reconstruction to register the pre-WI temperature conditions in Scotland, with Whitrig Bog in southern Scotland being the other (Brooks and Birks, 2001). Whitrig Bog displays a temperature of ~6 °C during the DS, broadly consistent with the reconstruction from Crudale Meadow given the estimated errors and differing training sets used.

T_{Jul} shows a strong rise into the start of the WI (CM-CZ2), reaching 11.5 ± 1.4 °C at 14 170 ± 140 cal a BP. Inferred temperatures then continue to rise to 12.8 ± 1.4 °C at 14 070 ± 70 cal a BP. T_{Jul} rose faster than $CaCO_3$, most likely due to a lag in landscape stability leading to inhibited authigenic carbonate precipitation.

Early Windermere Interstadial ACE (CM-CZ3) ~14 070 ± 70 to 13 960 ± 160 cal a BP

The onset of the Early WI event around 14.0 ka BP does not appear to be synchronous between both temperature proxies. Both T_{Jul} and $\delta^{18}O$ start to decline at 14 070 ± 70 cal a BP. However, T_{Jul} only shows a very minor decline from the

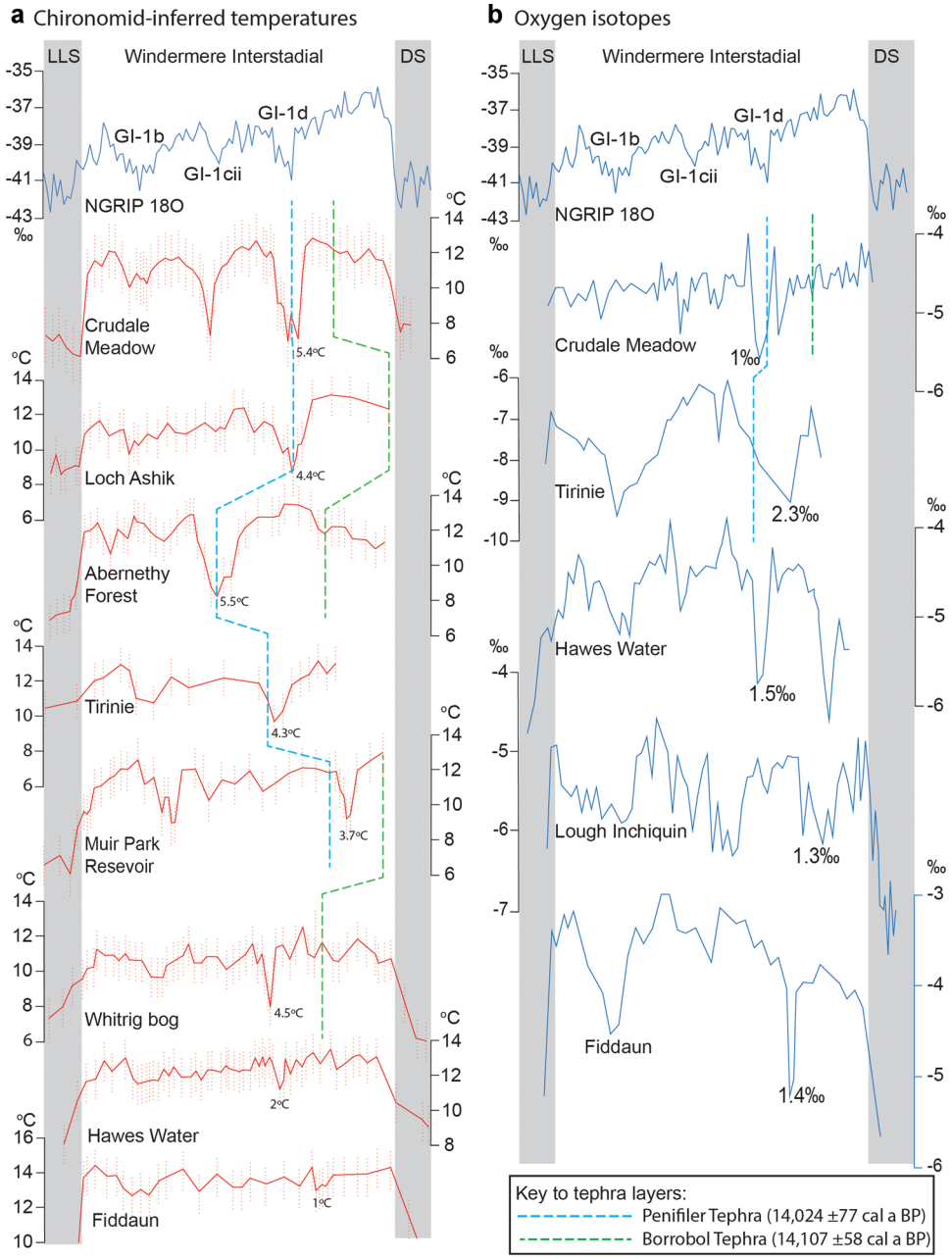

Figure 8. Comparison of the Crudale Meadow proxy records with other sites from the British Isles which are arranged latitudinally from north to south. (a) Comparison of the T_{Jul} record from Crudale Meadow with the NGRIP $\delta^{18}O$ record and with T_{Jul} records from other British and Irish sites with error estimates represented as dotted lines. All T_{Jul} records are plotted on a common *y*-axis scaling. (b) Comparison of the Crudale Meadow isotope record with the NGRIP $\delta^{18}O$ record and other $\delta^{18}O$ records from lacustrine sequences in Britain and Ireland. Note that all records, except those from Tirinie and NGRIP, are on a common *y*-axis scaling. Note that the *x*-axes in (a) and (b) are based on depth and stretched between records to allow comparison. Grey shaded areas denote the Dimlington Stadial (DS) and the Loch Lomond Stadial (LLS). References: NGRIP (Rasmussen *et al.*, 2014), Loch Ashik and Abernethy Forest (Brooks *et al.*, 2012), Tirinie (Abrook *et al.*, submitted; Candy *et al.*, 2016), Muir Park Reservoir (Brooks *et al.*, 2016), Whitrig Bog (Brooks and Birks, 2001), Hawes Water (Marshall *et al.*, 2002; Lang *et al.*, 2010), Fiddaun (van Asch *et al.*, 2012), Loch Inchiquin (Diefendorf *et al.*, 2006). [Color figure can be viewed at wileyonlinelibrary.com]

previous sample of 0.4 °C, well within the errors of the WA-PLS model, whereas $\delta^{18}O$ displays a much more substantial decline. T_{Jul} only starts to show a stronger decline in the following centimetre which has an age of 14 050 ± 80 cal a BP. As both proxies were sampled from the same core and same stratigraphic level, age-model errors cannot explain the difference between the two proxies. Therefore, approximately 20 years had elapsed between the decrease in $\delta^{18}O$ and the decline in chironomid-inferred T_{Jul}. This pattern is supported by the bulk lithological data which also show a decline in percentage $CaCO_3$ prior to a change in T_{Jul}. Palaeoecological proxies may display a lag in response to changes in environmental variables due to migration delay as well as physiological and metabolic processes of organisms buffering against environmental change (Słowiński *et al.*, 2017). This possible delay in chironomid response may have only been seen due to the application of high-resolution sampling (20 years/sample) at Crudale Meadow.

It is potentially possible that $\delta^{18}O$ does not record the full magnitude of temperature change. The isotopic value at 633 cm of -4.15% appears anomalously high and its position on the downward temperature trend may mean that the sample was affected by detrital contamination as vegetation broke down and landscape erosion increased. Therefore, it could be that minimum $\delta^{18}O$ values were attained at 633 cm, the same time as T_{Jul}, but were obscured due to detrital contamination. This would have consequences for the timing of when minimum temperatures were reached in both proxies. However, this cannot be explored further with the available data.

Later part of Windermere Interstadial and other ACEs (CM-CZ4 to CM-CZ7) ~13 960 ± 160 to 12 830 ± 500 cal a BP

During CM-CZ4, there was a decline in $\delta^{18}O$ with a magnitude of around 0.4%. However, there was no corresponding decline in T_{Jul}. Several factors may explain this. First, summer temperatures declined, but there was no response in the chironomids, either because the change in summer temperatures was not large enough to impact on chironomid ecology and/or ecological thresholds were not crossed. Second, winter temperatures may have declined, but no corresponding decline occurred in T_{Jul}, i.e. there was an increase in seasonality. Finally, factors other than temperature may have influenced the $\delta^{18}O$ signal, such as a change in moisture source (Rozanski *et al.*, 1992, 1993) or a shift in the seasonality of precipitation (Candy *et al.*, 2015). Additional measurements would be needed for such factors to be fully understood, e.g. n-alkanes or δD.

In CM-CZ5, a mid-WI ACE is detected with both proxies showing a decline in inferred temperatures. Minimum temperatures were attained synchronously at 13 670 ± 200 cal a BP, taking into account the sampling resolution employed. A late WI ACE occurs during CM-CZ7 with T_{Jul} and $\delta^{18}O$ showing a decline of 1 °C and 0.5%, respectively. As with the mid-WI ACE, the timing of event onset between both proxies is synchronous with respect to the sampling resolution, both showing declines at 13 330 ± 320 cal a BP. Minimum values are, however, attained first in the $\delta^{18}O$ record at 13 220 ± 400 cal a BP and later at 13 170 ± 420 cal a BP in the T_{Jul} record.

End of the Windermere Interstadial and onset of Loch Lomond Stadial (CM-CZ8 and -CZ9) ~12 990 ± 500 cal a BP

Temperatures increase briefly in CM-CZ8 before declining into CM-CZ9, with T_{Jul} falling to 6 ± 1.5 °C. The lack of $CaCO_3$ precipitation also suggests a very cold climate. Fragments of terrestrial moss and herbaceous material are found at 602 cm/12 800 ± 500 cal a BP, indicative of landscape erosion and in-wash of material.

In summary, the T_{Jul} and $\delta^{18}O$ records from the CRUM1 sequence indicates that multiple ACEs occurred during the WI in the northern British Isles. The clearest and most extreme of these is seen in CM-Z3, centred around ~14.0 ka BP, which has the strongest expression of any ACE in both proxies and is characterised by approximately 5.4 °C worth of cooling and 1% of isotopic decline. While the middle and late part of the WI are clearly characterised by other abrupt events, centred around ~13.6 ka BP and ~13.2 ka BP, respectively, neither of these are as pronounced as ~14.0 ka BP ACE.

Comparison with other records

The trends observed in the T_{Jul} and $\delta^{18}O$ records from Crudale Meadow are similar to those seen in other records around the North Atlantic region, with three centennial-scale ACEs punctuating the WI (e.g. Diefendorf *et al.*, 2006; Lang *et al.*, 2010; Brooks *et al.*, 2012) (Fig. 8). Many T_{Jul} and $\delta^{18}O$ records, including Crudale Meadow, have particularly good agreement with the pattern of temperature changes seen in the Greenland ice-core records (Lowe *et al.*, 2008; Rasmussen *et al.*, 2014). It is, therefore, tempting to correlate these cold oscillations observed in terrestrial records to the GI-1d, GI-1cii and GI-1b events; here we examine the validity of this notion.

Brooks and Langdon (2014) have previously synthesised T_{Jul} records from northwest Europe using time slices based on the GI-1 subdivisions with averaged reconstructed temperatures for each period. Here we build on their work by including more recent T_{Jul} reconstructions from Muir Park Reservoir (Brooks *et al.*, 2016) and Tirinie (Abrook *et al.*, 2020), and expanding the analysis to include $\delta^{18}O$ information. We restrict our analysis to reconstructions from the British Isles as these tend to provide high sample density reconstructions and robust chronological control. Particular attention is paid to the ACE centred on ~14.0 ka BP, where radiocarbon and tephra data provide a robust link between the records.

Early WI ACE ~14.0 ka BP (≈GI-1d)

The presence of the Borrobol and Penifiler Tephras at Crudale Meadow means that the large cooling event during CM-C3, the largest of the WI ACEs, with a cooling of 5.4 °C, can be constrained to ~14.0 ka BP with a high degree of certainty. This broadly correlates with the GI-1d cooling event expressed in Greenland (14 075 ± 169 to 13 954 ± 165 b2k; Rasmussen *et al.* 2014).

The Borrobol and Penifiler Tephras are also present in many other Scottish records and allow robust correlation of this event between sites. The majority of Scottish C-IT records also show this early WI ACE as being the largest ACE in terms of magnitude to punctuate the WI. However, there are large spatial differences in the magnitude of T_{Jul} for the ~14.0 ka BP event and a strong correlation with latitude is observed (Fig. 8a). Sites further north experience a far greater magnitude of cooling, e.g. Crudale Meadow and Loch Ashik (4.4 °C, 57°N, Brooks *et al.*, 2012), than those sites further south, e.g. Muir Park Reservoir (3.5 °C, 56°N, Brooks *et al.*, 2016). Sites in England (Hawes Water; 53°N; Lang *et al.*, 2010) and Ireland (Fiddaun; 54°N; Van Asch *et al.*, 2012) have less chronological certainty during the early WI as they do not contain the Borrobol and Penifiler Tephra. However, there is still evidence of an early WI ACE, which, based on the site chronologies, is also thought to occur at ~14.0 ka BP. Fiddaun has two

radiocarbon dates constraining an event at ~14.0 ka BP with a magnitude of 1 °C. Hawes Water relies on climatostratigraphy for dating events during the WI; however, an event early on in the WI has a magnitude of 2 °C and is the largest event present in the WI.

It is difficult to evaluate whether similar latitudinal trends were present in $\delta^{18}O$ records at ~14.0 ka BP due to the paucity of $\delta^{18}O$ records arranged along a north–south transect with sufficient sampling resolution, methodological controls, and chronological constraints. However, three records which lie between 54 and 52°N – Loch Inchiquin (Diefendorf *et al.*, 2006), Hawes Water (Marshall *et al.*, 2002) and Fiddaun (Van Asch *et al.*, 2012) – all show $\delta^{18}O$ shifts of -1.3%, -1.5% and -1.4%, respectively, for the event broadly constrained to ~14.0 ka BP. Further north at Tirinie, which lies at 56°N, the $\delta^{18}O$ record displays a much larger isotopic shift of ~2.32% (Candy *et al.*, 2016). The isotopic shift at Crudale Meadow of 1% is much smaller than that seen at the sites mentioned above and may be due to: (1) the westerly position of the site causing reduced seasonality; (2) the 'actual' minimum isotopic value being obscured by detrital contamination with the potential of in-washed material at 633 cm; or (3) the most northerly latitudes of the British Isles may have been affected by changes in moisture source and/or changes in winter temperatures may have been more subdued.

Additional spatial trends in the data were explored (altitude and longitude) but were found to not have significant correlations with the magnitude of the events identified. Therefore, for the ~14.0 ka BP event at least, a forcing mechanism must be acting that exerts a stronger influence from south to north than it does from west to east. To further our understanding of the spatial expression in the magnitude of temperature changes for the ~14.0 ka BP event, a greater density of records is needed over longer north–south and east–west transects.

Other events in the Windermere Interstadial

The Crudale Meadow record, as well as other T_{Jul} and $\delta^{18}O$ records from Scotland and northern England, display several other ACEs in the middle and later parts of the WI. The comparison of these ACEs between sites is problematic for two reasons. Firstly, the lack of tephra marker layers and radiocarbon dates means definitive correlation of ACEs is not possible. Age models have error estimates of up to ±400 years which are as large or larger than the duration of the known ACEs in this period (Rasmussen *et al.*, 2014). Our chronological precision does not permit detailed comparisons of the timing of onset, duration and recovery from these later events, while in some cases the magnitudes of change are in the order of 1–3 °C, which is less than the cooling experienced at ~14.0 ka BP and similar to the predictive powers of the WA-PLS model. Despite these limitations, we suggest that broad-scale comparisons between records provide useful information on mid- to late WI variability.

A mid-WI event (often correlated to GI-1cii; 13 660–13 600 GICC05 yrs) is recorded in many records as the smallest of the WI ACEs (Brooks and Birks, 2000; Lang *et al.*, 2010; Brooks *et al.*, 2012). However, at Crudale Meadow, the mid-WI event is the second largest ACE with a magnitude similar to that seen

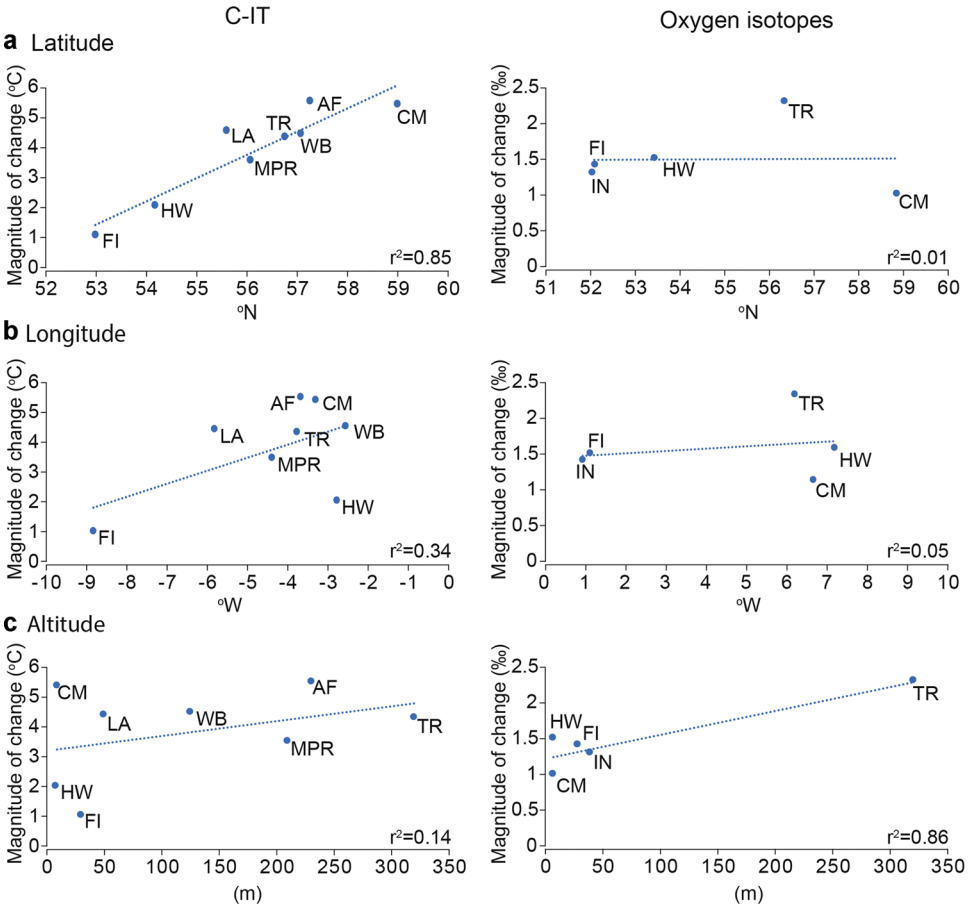

Figure 9. Magnitude in T_{Jul} and $\delta^{18}O$ for the 14.0 ka event from British and Irish records compared with (a) Latitude, (b) Longitude and (c) Altitude. Site abbreviations: AF (Abernethy Forest; Brooks *et al.*, 2012), CM (Crudale Meadow; this study), FI (Fiddaun; van Asch *et al.*, 2012), HW (Hawes water; Marshall *et al.*, 2002; Lang *et al.*, 2010), LA (Loch Ashik; Brooks *et al.*, 2012), LI (Loch Inchiquin; Diefendorf *et al.*, 2006), MPR (Muir Park Reservoir; Brooks *et al.*, 2016), TR (Tirinie; Candy *et al.*, 2016; Abrook, *et al.*, 2020), WB (Whitrig Bog; Brooks and Birks, 2001). [Color figure can be viewed at wileyonlinelibrary.com]

in the ~14.0 ka BP event with T_{Jul} displaying a decline of 3.9 °C and $\delta^{18}O$ decreasing by 0.7%. Currently, the large magnitude of this ACE in the Crudale Meadow sequence is difficult to reconcile and requires further testing at other locations to determine whether this is a local phenomenon specific to Crudale, the Orkney Islands, or whether it may be observed more widely. It may be that this event is very short-lived which has meant that it has been neglected due to the lower sampling resolution employed in previous chironomid studies missing this change. Alternatively, it may reflect a lower stratigraphic resolution in previous studies which has led to a mixing of adjacent warm and cold taxa, seemingly reducing its magnitude.

A later WI event (often correlated with GI-1b; 13 311–13 099 GICC05 yrs b2k) is infrequently recognised in isotope and T_{Jul} records across Britain with its best expression and dating seen at Tirinie (Candy *et al.* 2016; Abrook *et al.* 2020), where an event dated to between 13.45 and 13.02 cal a BP is defined by a decline of 1.8 °C T_{Jul} and an isotopic depletion of -2.9%. Other sites around Scotland, e.g. Whitrig Bog (Brooks and Birks, 2000), Loch Ashik and Abernethy Forest (Brooks *et al.*, 2012) and Muir Park Reservoir (Brooks *et al.*, 2016), record a late WI drop in T_{Jul} temps ranging from 2 to 3.5 °C and if these are registering the same event it would indicate that Crudale does not support this degree of cooling. This event appears to have a duration of ~450 years (at Tirinie) so it seems unlikely that low sampling resolution is a factor in its identification or characterisation. Therefore, where this late WI event is poorly represented or absent, it would suggest that the individual site records have suffered from either: (1) low stratigraphic resolution; (2) an alteration to the proxy signal from sediment mixing or reworking; and/or (3) overriding influence of site-specific factors.

Forcing mechanisms

At present, this study can only present the pattern of variability seen in ACEs in WI/GI-1; it is not possible to confidently ascribe a single forcing mechanism to them. However, the fact that such a large latitudinal gradient in response to the 14.0 ka BP/GI-1d oscillation existed and indicates that whatever drives this event has a greater influence at higher latitudes. As such, it is likely that ocean forcing plays a key role in triggering the cooling (McManus *et al.*, 2004). Changes in the strength of Atlantic Meridional Overturning Circulation (AMOC) are likely to be more strongly expressed in higher latitudes as these regions are more dependent upon the heat delivered by this circulation to maintain temperatures (e.g. Zhang, 2010). If a decline in AMOC strength was the driver of this event then it would, therefore, be reasonable to expect the northern parts of the British Isles to be most affected. While it is beyond the scope of this study to prove such mechanisms, the construction of transects of sites that span key latitudinal belts, as shown above, is a key means of generating empirical data against which model results can be validated.

Conclusion

The new high-resolution T_{Jul} and $\delta^{18}O$ records covering the WI from Crudale Meadow provide important insights into temperature changes for northern Britain. The data generated in this study allow the following conclusions to be drawn:

(1) An ACE centred on ~14.0 ka BP is clearly present in the CRUM1 sequence with a magnitude in the order of 5.4 °C. This event is bracketed by the Borrobol and Penifiler Tephras which suggests that it is broadly correlative to the GI-1d oscillation observed within the Greenland ice-core records.
(2) Although in a spatially restricted area of northwestern Europe, the magnitude of the temperature change of the 14.0 ka BP event across the northern British Isles suggests that latitude plays an important role. The correlation between summer temperature and latitude that existed at the peak of this event could potentially occur in future ACEs caused by the melting of the Greenland ice sheet due to anthropogenic global warming.
(3) Two later ACEs centred around ~13.6 ka BP and ~13.2 ka BP, of smaller magnitude than the ~14.0 ka BP oscillation, are present at Crudale Meadow. These seem to broadly equate with GI-1cii and GI-1b seen in Greenland. However, the chronological uncertainty across these parts of the sequence means these attributions are not certain. Additional chronological control is required to fully explore these events at Crudale and other locations in northwestern Europe.
(4) Crudale Meadow is the second record from Scotland to quantifiably record the onset of warming during the WI. It, and Whitrig Bog in southern Scotland, demonstrate ice-free conditions at their respective locations prior to WI warming; something not seen in other locations. Both sites have considerable potential to constrain climatic events over the WI and demonstrate the climatic differences recorded between two geographically near locations (Fig. 9).

Supporting information

Additional supporting information may be found in the online version of this article at the publisher's web-site.

Supporting information 1 – chironomid sample preparation procedure tests

Supporting information 2 – chironomid-inferred temperature reconstruction and validation statistics using the Norwegian calibration dataset

Acknowledgements and funding. Thanks go to the Quaternary Research Association (QRA) and their funding of a 'New Research Workers Award' to RT, which supported the fieldwork costs for this research. The authors are also grateful to Professor Oliver Heiri and coworkers for making the combined Norwegian–Swiss calibration dataset available. Finally, CF would like to thank Dr Marta Perez-Fernandez and Mr Iñaki Valcarcel for laboratory and technical assistance. CF was funded by the Natural Environmental Research Council, Grant no. NE/L002485/1.

Data availability statement

All data published in this paper are freely accessible in the Neotoma database.

References

Abrook AM, Matthews IP, Milner AM *et al.* 2020. Climatic drivers and environmental responses linked to abrupt climate events during the Last Glacial-Interglacial Transition in north-west Europe. *Quaternary Science Reviews* **250:** 106634.

Bennett KD. 1996. Determination of the number of zones in a biostratigraphical sequence. *New Phytologist* **132**(1): 155–170.

Birks HJB. 1998. Deevey Review 1: Numerical tools in palaeolimnology - progress, potentialities, and problems. *Journal of Paleolimnology* **20**: 307–332.

Birks HJB, Line JM, Juggins S *et al.* 1990. Diatoms and pH reconstruction. *Philosophical Transactions of the Royal Society of London B* **327**: 263–278.

Björck S, Walker MJC, Cwynar LC *et al.* 1998. An event stratigraphy for the last termination in the North Atlantic region based on the Greenland ice-core record: a proposal by the INTIMATE group. *Journal of Quaternary Science* **13**: 283–292.

Blockley S, Candy I, Matthews I *et al*. 2018. The resilience of postglacial hunter-gatherers to abrupt climate change. *Nature Ecology & Evolution* **2**: 810–818.

Brodersen KP, Lindegaard C. 1999. Classification, assessment and trophic reconstruction of Danish lakes using chironomids. *Freshwater Biology* **42**: 143–157.

Brodersen KP, Odegaard BV, Vestergaard O *et al*. 2001. Chironomid stratigraphy in the shallow and eutrophic Lake Søbygaard, Denmark: chironomid–macrophyte co-occurrence. *Freshwater Biology* **46**: 253–267.

Brodin YW. 1986. The postglacial history of Lake Flarken, southern Sweden, interpreted from subfossil insect remains. *Internationale Revue der Gesamten Hydrobiologia* **71**: 371–432.

Brodin Y-W, Gransberg M. 1993. Responses of insects, especially Chironomidae (Diptera), and mites to 130 years of acidification in a Scottish lake. *Hydrobiologia* **250**: 201–212.

Bronk Ramsey C. 2008. Deposition models for chronological records. *Quaternary Science Reviews* **27**(1–2): 42–60.

Bronk Ramsey C. 2009. Bayesian analysis of radiocarbon dates. *Radiocarbon* **51**(1): 337–360.

Brooks SJ, Birks HJB. 2000. Chironomid-inferred Late-glacial air temperatures at Whitrig Bog, southeast Scotland. *Journal of Quaternary Science* **15**(8): 759–764.

Brooks SJ, Birks HJB. 2001. Chironomid-inferred air temperatures from Lateglacial and Holocene sites in north-west Europe: progress and problems. *Quaternary Science Reviews* **20**(16): 1723–1741.

Brooks SJ, Langdon PG. 2014. Summer temperature gradients in northwest Europe during the Lateglacial to early Holocene transition (15-8 ka bp) inferred from chironomid assemblages. *Quaternary International* **341**: 80–90.

Brooks SJ, Davies KL, Mather KA *et al*. 2016. Chironomid inferred summer temperatures for the Last Glacial–Interglacial Transition from a lake sediment sequence in Muir Park Reservoir, west-central Scotland. *Journal of Quaternary Science* **31**(3): 214–224.

Brooks SJ, Langdon PG, Heiri O. 2007. *The identification and use of Palaearctic Chironomidae larvae in Palaeoecology*. QRA Technical Guide No. 10. Quaternary Research Association: London.

Brooks SJ, Matthews IP, Birks HH *et al*. 2012. High resolution Late-Glacial and early Holocene summer air temperature records from Scotland inferred from chironomid assemblages. *Quaternary Science Reviews* **41**: 67–82.

Brundin L. 1956. Die bodenfaunistischen Seetypen und ihre Anwendbarkeit auf die Südhalbkugel. Zugleich eine Theorie der produktionsbiologischen Bedeutung der glazialen Erosion. *Report of the Institute of Freshwater Research. Drottningholm* **37**: 186–235.

Bunting MJ. 1994. Vegetation history of Orkney, Scotland: pollen records from two small basins in west Mainland. *New Phytology* **128**: 771–792.

Candy I, Abrook A, Elliot F *et al*. 2016. Oxygen isotopic evidence for high-magnitude, abrupt climatic events during the Lateglacial Interstadial in north-west Europe: analysis of a lacustrine sequence from the site of Tirinie, Scottish Highlands. *Journal of Quaternary Science* **31**(6): 607–621.

Candy I, Farry A, Darvill CM *et al*. 2015. The evolution of Palaeolake Flixton and the environmental context of Star Carr: An oxygen and carbon isotopic record of environmental change for the early Holocene. *Proceedings of the Geologists' Association* **126**(1): 60–71.

Cranston PS. 1982. A Key to the Larvae of the British Orthocladiinae (Chironomidae). Freshwater Biological Association: Ambleside.

Cranston PS, Oliver DR, Saether OA. 1983. The larvae of Ortocladiinae (Diptera, Chironomidae) of the Holarctic region – Keys and diagnoses. In *Chironomidae of the Holartic region – Keys and diagnoses. Part 1. Larvae. Entomologica Scandinavica*, Wiederholm T (ed.). Supplement 19: 149–291.

Diefendorf AF, Patterson WP, Mullins HT *et al*. 2006. Evidence for high-frequency late Glacial to mid-Holocene (16 800 to 5500 cal a B.P.) climate variability from oxygen isotope values of Lough Inchiquin, Ireland. *Quaternary Research* **65**: 78–86.

Engels S, Cwynar LC. 2011. Changes in fossil chironomid remains along a depth gradient: evidence for common faunal breakpoints within lakes. *Hydrobiologia* **665**: 15–38.

Engels S, Heiri O, Medeiros AS *et al*. 2020. Temperature change as a driver of spatial patterns and long - term trends in chironomid (Insecta: Diptera) diversity. *Global Change Biology* **26**: 1155–1169.

Engels S, Helmens KF, Väliranta M *et al*. 2010. Early Weichselian (MIS-5d and 5c) temperatures and environmental changes as recorded by chironomids and macroremains at Sokli (northern Fennoscandia). *Boreas* **39**: 689–704.

Gale S, Hoare P. 1991. Quaternary Sediments: Petrographic Methods for the Study of Unlithified Rocks. Belhaven and Halsted Press: New York; 323.

Gregory JM, Dixon KW, Stouffer RJ. 2005. A model intercomparison of changes in the Atlantic thermohaline circulation in response to increasing atmospheric CO2 concentration. *Geophysical Research Letters* **32**: L12703.

Grimm EC. 1987. CONISS: a FORTRAN 77 program for stratigraphically constrained cluster analysis by the method of incremental sum of squares. *Computers and Geosciences* **13**: 13–35.

Hawkins E, Smith RS, Allison LC. 2011. Bistability of the Atlantic overturning circulation in a blobal climate model and links to ocean freshwater transport. *Geophysical Research Letters* **38**: L1065.

Heiri O, Lotter AF. 2001. Effect of low count sums on quantitative environmental reconstructions: an example using subfossil chironomids. *Journal of Paleolimnology* **26**: 343–350.

Heiri O, Lotter AF, Lemcke G. 2001. Loss on ignition as a method for estimating organic and carbonate content in sediments: reproducibility and comparability of results. *Journal of Paleolimnology* **25**: 101–110.

Heiri O, Brooks SJ, Birks HJB *et al*. 2011. A 274-lake calibration dataset and inference model for chironomid-based summer air temperature reconstruction in Europe. *Quaternary Science Reviews* **30**: 3445–3456.

Hill MO. 1973. Diversity and evenness: a unifying notation and its consequences. *Ecology* **54**: 427–432.

Juggins S. 2007. C2 Version 1.7.7. Software for ecological and palaeoecological data analysis and visualisation. Newcastle upon Tyne: Newcastle University. [Software]

Juggins S. 2017. rioja: Analysis of Quaternary Science Data, R package version 0.9-21. [Software] http://cran.r-project.org/package=rioja

Kansanen P. 1985. Assessment of pollution history from recent sediments in Lake Vanajavesi, Southern Finland. 2. Changes in the Chironomidae, Chaoboridae and Ceratopogonidae (Diptera) fauna. *Annales Zoologici Fennici* **22**(1): 57–90.

Kearney R, Albert PG, Staff RA. 2018. Ultra-distal fine ash occurrences of the Icelandic Askja-S Plinian eruption de- posits in Southern Carpathian lakes: new age constraints on a continental scale tephrostratigraphic marker. *Quaternary Science Reviews* **188**: 174–182.

Lang B, Brooks SJ, Bedford A *et al*. 2010. Regional consistency in Lateglacial chironomid-inferred temperatures from five sites in north-west England. *Quaternary Science Reviews* **29**: 1528–1538.

Leng MJ, Marshall JD. 2004. Palaeoclimate interpretation of stable isotope data from lake sediment archives. *Quaternary Science Reviews* **23**(7): 811–831.

Lowe JJ, Ammann B, Birks HH *et al*. 1994. Climatic changes in areas adjacent to the North Atlantic during the last glacial-interglacial transition (14–9 ka bp): a contribution to IGCP-253. *Journal of Quaternary Science* **9**: 185–198.

Lowe JJ, Birks HH, Brooks SJ *et al*. 1999. The chronology of palaeoenvironmental changes during the Last Glacial-Holocene transition: towards an event stratigraphy for the British Isles. *Journal of the Geological Society* **156**(2): 397–410.

Lowe JJ, Rasmussen SO, Björck S *et al*. 2008. Synchronisation of palaeoenvironmental events in the North Atlantic region during the Last Termination: a revised protocol recommended by the INTIMATE group. *Quaternary Science Reviews* **27**(1–2): 6–17.

Lowe JJ, Walker MJC. 1977. The reconstruction of the Lateglacial environment in the southern and eastern Grampian Highlands. In *Studies in the Scottish Lateglacial Environment*, Gray JM, Lowe JJ (eds). Pergamon Press: Oxford; 101–118.

Marshall JD, Jones RT, Crowley SF *et al*. 2002. A high resolution Late-Glacial isotopic record from Hawes Water, north-west England: climatic oscillations: calibration and comparison of palaeotempera-

ture proxies. *Palaeogeography, Palaeoclimatology, Palaeoecology* **185**(1): 25–40.

Massaferro J, Brooks SJ. 2002. Response of chironomids to late quaternary environmental change in the Taitao Peninsula, Southern Chile. *Journal of Quaternary Science* **17**(2): 101–111.

McManus JF, Francois R, Gherardi JM *et al*. 2004. Collapse and rapid resumption of Atlantic meridional circulation linked to deglacial climate changes. *Nature* **428**: 834–837.

Moar NT. 1969. Two pollen diagrams from the mainland, Orkney islands. *New Phytology* **68**: 201–208.

Moller Pillot HKM. 2009. *Chironomidae larvae. Volume 2: Biology and ecology of the Chironomini*. KNNV Publishing: Zeist.

Moller Pillot HKM. 2013. *Chironomidae larvae. Volume 3: Biology and ecology of the aquatic Orthocladiinae*. KNNV Publishing: Zeist.

Mykura W, Flinn D, May F. 1976. *British Regional Geology: Orkney and Shetland. Institute of Geological Sciences Memoir*. HMSO: Edinburgh

Oksanen J, Blanchet FG, Friendly M *et al*. 2017. Package 'vegan': community ecology package, version:2.4-4.

Palmer AP, Matthews IP, Candy I *et al*. 2015. The evolution of Palaeolake Flixton and the environmental context of Star Carr, NE. Yorkshire: Stratigraphy and sedimentology of the Last Glacial-Interglacial Transition (LGIT) lacustrine sequences. *Proceedings of the Geologists' Association* **126**(1): 50–59.

Petoukhov V, Claussen M, Berger A. 2005. EMIC Intercomparison Project (EMIP–CO2): Comparative analysis of EMIC simulations of climate, and of equilibrium and transient responses to atmospheric CO2 doubling. *Climate Dynamics* **25**: 363–385.

Quinlan R, Smol JP. 2001. Chironomid-based inference models for estimating end-of-summer hypolimnetic oxygen from south-central Ontario shield lakes. *Freshwater Biology* **46**: 1529–1551.

R core Team. 2018. R: A language and environment for statistical computing. R Foundation for statistical Computing, Vienna, Austria. https://www.R-project.org/

Rasmussen SO, Andersen KK, Svensson AM *et al*. 2006. A new Greenland ice core chronology for the last glacial termination. *Journal of Geophysical Research: Atmospheres* **111**(D6).

Rasmussen SO, Bigler M, Blockley SP *et al*. 2014. A stratigraphic framework for abrupt climatic changes during the Last Glacial period based on three synchronized Greenland ice-core records: refining and extending the INTIMATE event stratigraphy. *Quaternary Science Reviews* **106**: 14–28.

Reimer P, Austin W, Bard E *et al*. 2020. The IntCal20 Northern Hemisphere Radiocarbon Age Calibration Curve (0–55 cal kbp). *Radiocarbon* **62**(4): 725–757.

Rieradevall M, Brooks SJ. 2001. An identification guide to subfossil Tanypodinae larvae (Insecta: Diptera: Chironomidae) based on sephalic setation. *Journal of Paleolimnology* **25**: 81–99.

Rozanski K, Araguás-Araguás L, Gonfiantini R. 1992. Relation between long-term trends of oxygen-18 isotope composition of precipitation and climate. *Science* **258**: 981–985.

Rozanski K, Araguás-Araguás L, Gonfiantini R. 1993. Isotopic patterns in modern global precipitation. In *Climate Change in Continental Isotopic Records*, Swart PK, Lohmann KC, McKenzie J, Savin S (eds). American Geophysical Union: Washington, DC; 1–36.

Simpson G. 2020. Analogue: Analogue and Weighted Averaging Methods for Palaeoecology. R package version (0.17-4).

Słowiński M, Zawiska I, Ott F *et al*. 2017. Differential proxy responses to late Allerød and early Younger Dryas climatic change recorded in varved sediments of the Trzechowskie palaeolake in Northern Poland. *Quaternary Science Reviews* **158**: 94–106.

Talbot MR. 1990. A review of the palaeohydrological interpretation of carbon and oxygen isotopic ratios in primary lacustrine carbonates. *Chemical Geology: Isotope Geoscience Section* **80**: 261–279.

Telford R. 2014a. Analogue quality, reconstruction quality. [Blog] *Musings on Quantitative Palaeoecology*. https://quantpalaeo.wordpress.com/2014/05/11/analogue-quality-reconstruction-quality/ [Accessed June 2020].

Telford R. (2014b). Beyond nearest analogue distance. [Blog] *Musings on Quantitative Palaeoecology*. https://quantpalaeo.wordpress.com/2014/05/17/beyond-nearest-analogue-distance/ [Accessed June 2020].

ter Braak, C. 1986 Canonical Correspondence Analysis: A New Eigenvector Technique for Multivariate Direct Gradient Analysis. *Ecology* **67**(5): 1167–1179.

ter Braak CJF, Juggins S. 1993. Weighted averaging partial least squares regression (WA-PLS): an improved method for reconstructing environmental variables from species assemblages. *Hydrobiologia* **269**(270): 485–502.

ter Braak CJF, Juggins S, Birks HJB *et al*. 1993. Weighted averaging partial least squares regression (WA-PLS): definition and comparison with other methods for species-environment calibration. In *Multivariate Environmental Statistics*, Patil GP, Rao CR (eds). Elsevier: Amsterdam; 525–560.

Timms RGO, Matthews IP, Palmer AP *et al*. 2018. Toward a tephrostratigraphic framework for the British Isles: A Last Glacial to Interglacial Transition (LGIT c. 16-8 ka) case study from Crudale Meadow, Orkney. *Quaternary Geochronology* **46**: 28–44.

Troels-smith J. 1955. karakterisering af lose jordarter danmarks geologiske undersogelse series IV. **3(10): 73**.

Vallenduuk HJ, Moller Pillot HKM. 2007. *Chironomidae larvae of the Netherlands and adjacent lowlands. General Ecology and Tanypodinae*. KNNV Publishing: The Netherlands.

van Asch N, Lutz AF, Duijkers MC *et al*. 2012. Rapid climate change during the Weichselian Late-Glacial in Ireland: chironomid-inferred summer temperatures from Fiddaun, Co. Galway. *Palaeogeography, Palaeoclimatology, Palaeoecology* **315–316**: 1–11.

Whittington G, Edwards KJ, Zanchetta G *et al*. 2015. Lateglacial and early Holocene climates of the Atlantic margins of Europe: Stable isotope, mollusc and pollen records from Orkney, Scotland. *Quaternary Science Reviews* **122**: 112–130.

Wiederholm T (ed). 1983. Chironomidae of the Holarctic region. Keys and Diagnoses. Part I. *Larvae: Entomologica Scandinavia Supplement* 19: 1–457.

Zhang R. 2010. Latitudinal dependence of Atlantic meridional overturning circulation (AMOC) variations. *Geophysical Research Letters* **37**: L16703.